Published in final edited form as:
Muscle Nerve. 2014 March ; 49(3): 378–388. doi:10.1002/mus.23924.

The mERG1a Channel Modulates Skeletal Muscle *MuRF1*, but not *MAFbx*, Expression

Amber L. Pond, PhD[1,2], **Carrie Nedele, DVM**[3], **Wen-Horng Wang, PhD**[2], **Xun Wang, PhD**[3], **Claire Walther, DVM**[3], **Christine Jaeger, PhD**[3], **Kevin S. Bradley, HS**[1], **Huahua Du, PhD**[4], **Naoya Fujita, PhD**[5], **Greg H. Hockerman, PhD**[2], and **Kevin M. Hannon, PhD**[3]

[1]Anatomy Dept., Southern Illinois University School of Medicine, Carbondale, IL

[2]Medicinal Chemistry and Molecular Pharmacology, School of Pharmacy, Purdue University, West Lafayette, IN

[3]Basic Medical Sciences, School of Veterinary Medicine, Purdue University, West Lafayette, IN

[4]Feed Science Institute, Zhejiang University, Hangzhou, PR China

[5]Cancer Chemotherapy Center, Japanese Foundation for Cancer Research, Tokyo 135-8550, Japan

Abstract

Introduction—The mechanism by which the mERG1a K^+ channel increases ubiquitin proteasome proteolysis (UPP) was investigated.

Methods and Results—Atrophic gastrocnemius muscles of hindlimb suspended mice express *mERG1a, MuRF1* and *MAFbx* genes. Electro-transfer of *mERG1a* into non-suspended mouse muscle significantly decreases muscle fiber size (12.6%) and increases UPP E3ligase MuRF1 mRNA (real time PCR; 2.1 fold) and protein (immunoblot; 23.7%), but does not affect MAFbx E3ligase expression. Neither mERG1a-induced decreased fiber size nor mERG1a-induced increased *MuRF1* expression is significantly curtailed by co-expression of inactive *HR-FOXO3a*, a gene encoding a transcription factor known to induce *MAFbx* expression by binding directly to its promoter.

Discussion—The mERG1a K^+ channel significantly increases expression of *MuRF1* but not *MAFbx*. We explored this expression pattern by ectopically expressing an inactive *FOXO3a* and showing that it is not involved in mERG1a-mediated expression of *MuRF1*. These findings suggest that mERG1a does not modulate *MuRF1* expression through the AKT/FOXO pathway.

Keywords

mERG1a; Skeletal Muscle Atrophy; Ubiquitin Proteasome Proteolysis; *MuRF1*; *MAFbx*; Atrogin1

Corresponding Author: Amber Pond, Anatomy Dept., Southern Illinois University School of Medicine, 2080 Life Sciences III, 1135 Lincoln Drive, Carbondale, IL 62901.

INTRODUCTION

Skeletal muscle (SKM) comprises 35–45% of the human body mass and is necessary for movement, posture, support, and temperature regulation. SKM atrophy, a loss in muscle mass and strength, can be induced by numerous stimuli: disease (e.g., cancer cachexia, sepsis, HIV/AIDS, diabetes), injury (spinal cord damage, denervation), immobilization, fasting, ageing and glucocorticoid treatment[1,2]. Muscle loss is attributable to either a decreased protein synthesis, increased protein degradation or some combination of both of these events. The extent to which each contributes to muscle loss varies with animal model, the evoking stimulus, study time course and muscle fiber type[2,3,4]. The protein degradation that produces atrophy results primarily from the activity of 3 proteolytic systems: calpains, cathepsins, and the ubiquitin proteasome pathway (UPP). It is reported that the UPP is the primary proteolytic system involved[5] and is purported to be responsible for as much as 75% of the protein degradation that occurs during SKM atrophy[1,6,7]. The UPP is a multistep pathway requiring activation of a ubiquitin protein by a ubiquitin-activating enzyme (E1) and ATP hydrolysis. The activated ubiquitin is transferred to the ubiquitin-carrier protein (E2), which binds to a ubiquitin protein ligase (E3 ligase) carrying a protein substrate. The E3 ligase then transfers the ubiquitin to the targeted substrate. Once a substrate carries (a minimum of 4) ubiquitin molecules, it is degraded by the 26S proteasome[1,6,7]. The basic mechanistic nature of the UPP has been described, but the specific players vary, as do the signaling pathways that lead to transcription and translation of these players. To date, 2 muscle specific ubiquitin E3 ligases have been described: Atrogin1 (protein product of Muscle atrophy F-box, *MAFbx*, gene) and Muscle RING Finger-1 (MuRF1). *MAFbx*/Atrogin1 is a member of the SCF (Skp1, cdc53/Cullin and F-box protein) subfamily of ligases, containing an F-box domain which serves to bind the E3 complex to a targeted protein[8,9,10]. MuRF1 belongs to the RING Finger E3 ligase subfamily which has a canonical N-terminal RING domain followed by a conserved region characteristic of the MuRF1 family and a zinc-finger domain[8,11]. Expression of these E3 ligases has been shown to be modulated variably by both the PI3K/AKT/FOXO and the IKK-β/IκB-α/Nfkappa B (NF-κB) pathways, dependent upon animal model and the stimulus inducing the atrophic state[1,2,6,7]. It has recently been shown that these 2 pathways are responsible for roughly half each of the muscle wasting that occurs in immobilization-induced SKM atrophy, demonstrating that they are the main pathways involved in this type of atrophy[12].

The ether-a-gogo-related gene 1a (*ERG1a*) K^+ channel (Kv11.1, KCNH) produces the I_{Kr} current which is partially responsible for late phase repolarization of the cardiac action potential. Mutations in this channel have been linked with Long QT Syndrome 2 (LQT2), a cardiac disorder characterized clinically by a prolonged QT interval, *torsade de pointes*, and sudden cardiac death[13]. Two alternative splice variants of *ERG1* have been cloned from human (*HERG1A* and *1B*[14]) and mouse (*mERG1a* and *1b*[15]) cDNA libraries, and high levels of *ERG1a* and *1b* expression have been detected in heart and brain of various mammals, including rats, mice and humans[14,15,16]. In previous studies with mice, we showed that the mERG1a homomultimeric channel is linked to SKM atrophy induced by hindlimb suspension (HS; i.e., an unloading model) and cancer cachexia[17]. Specifically, we showed that: 1) mERG1a channel protein level is upregulated in the gastrocnemius muscles (GM) of

hindlimb suspended mice experiencing atrophy relative to matched muscles in weight bearing (WB) control mice; 2) ectopic expression of the wildtype (WT) *mERG1a* splice variant in SKM of WB mice induced atrophy while co-expression of the WT and a dominant negative *mERG1a* subunit (*DN-mERG1a*, G628S[18]) blocked atrophy in these mice; 3) ectopic expression of the *DN-merg1a* mutant in hindlimb suspended mice inhibited atrophy; 4) pharmacological block of *mERG1a* inhibited atrophy in hindlimb suspended mice and increased muscle fiber cross sectional area (CSA) in WB mice; and 5) ectopic expression of the WT *mERG1a* channel in mouse GM increased UPP activity.

Here we investigate the mechanism by which *mERG1a* modulates the UPP. Using a mouse HS model of atrophy, our studies begin with a time course which demonstrates that our HS model indeed induces increased expression of the *mERG1a* gene and also *MuRF1* and *MAFbx* genes encoding E3 ligases while, interestingly, electro-transfer[17,19] of *mERG1a* into mouse GM induces expression of the *MuRF1*, but not the *MAFbx* gene. These results are confirmed with immunoblot studies showing that MuRF1 and Atrogin1 protein levels are increased in response to HS, but that only MuRF1 protein levels increase in response to ectopic expression of *mERG1a*. We confirm that *mERG1a* expression is not modulating *MAFbx* transcription by ectopically co-expressing *mERG1a* and a *MAFbx*/Atrogin1 luciferase reporter[20] and showing that *mERG1a* expression does not increase *MAFbx* promoter-driven luciferase activity levels. Additionally, we co-expressed genes encoding *mERG1a* and *FOXO3a*, a transcription factor shown to induce expression of both *MAFbx* and *MuRF1* genes in some models of atrophy[20,21], and demonstrate that *mERG1a* expression does not modulate *MuRF1* (or *MAFbx*) transcription through *FOXO3a* expression.

MATERIALS AND METHODS

Animals

All procedures were approved by the Purdue Animal Care and Use Committee. Seven- to 8-week old ND4-Swiss Webster male mice (Harlan-Sprague; Indianapolis, IN) were used in all procedures. Animals were housed in Purdue University facilities on a 12 hour light/dark cycle, monitored by lab animal veterinarians and provided food and water *ad libitum*.

Hindlimb Suspension (HS)

Custom suspension cages were constructed as described previously[22]. Mice were placed in these cages resting in approximately a 30° head down tilt with their hindlimbs elevated so that they were unable to place any load on the hindlimbs. Control mice were kept in commercial mouse cages in a normal weight bearing state.

Tissue Sectioning, Staining and CSA Determination

GMs were embedded, cryo-sectioned (12 μm) and stained for β–galactosidase (lacZ) activity as described earlier[17]. Images of sections were captured with a Leaf Micro–Lumina digital camera (Scitex; Tel-Aviv, Israel). The CSA (μm^2) of each muscle fiber was determined using Image J (NIH; Bethesda, MD).

Plasmids

The *mERG1a* clone in pBK/CMV[15] and the dominant negative *mERG1a* (*DN-mERG1a*) clone in pBK/CMV[18] were generous gifts from Dr. Barry London (Cardiovascular Institute, University of Pittsburgh, PA). The CMV-*lacZ* in pNL vector was purchased from the Center Commercial de Gros (Toulouse, France). The phRL synthetic *Renilla* luciferase reporter vector was purchased from ProMega (Madison, WI). The *MAFbx*/Atrogin1 luciferase reporter was generously provided by Dr. Stewart Lecker (Beth Israel Deaconess Medical Center, Boston, MA[20]). The *HR-FOXO3a* (*H212R*) plasmid, a mutated form of *FOXO3a* which is inactive because of its inability to bind DNA, was developed in the laboratory of Dr. Naoya Fujita (Japanese Foundation for Cancer Research, Japan[23]).

Electro-transfer

Mice were anesthetized with 10 μl/g body weight of a solution of xylazine (1 mg/ml) and ketamine (9 mg/ml) in sterile saline. GMs of shaved hindlimbs were injected with expression plasmids in 50 μl sterile saline and electroporated with 8 pulses at 200V/cm for 20 ms at 1 Hertz with an ECM 830 ElectroSquare Porator (BTX; Hawthorne, NY). This method has been shown to result in gene transcription and translation in SKM in our laboratory[17,19].

Real time PCR

Trizol reagent (Invitrogen; Carlsbad, CA) was used to extract total RNA from SKM according to manufacturer's instructions. The extraction was followed sequentially by phenol/chloroform extraction and ethanol precipitation. Any contaminating DNA was degraded by 2 10-min treatments with DNase I (ProMega; Madison, WI). DNase was then heat inactivated. SYBR Green Supermix with Rox (Applied Biosystems; Foster City, CA) was added to the PCR reaction (per manufacturer's instructions), and finally primers (see Table 1) for the gene of interest were added to the samples (in triplicate), while primers for an appropriate "housekeeping" gene (the *18S ribosomal subunit*) were added to duplicate samples (in triplicate). A 7300 Real Time PCR System (Applied Biosystems) was used to detect SYBR Green fluorescence as a measure of amplicon. Sample C_T values were normalized to (subtracted from) the C_T values of the "housekeeping" gene, and the number 2 was raised to a power equal to the difference between the sample C_T values of the *18S subunit* and the gene of interest.

Dual Luciferase Reporter Assay

The Dual-Luciferase Reporter Assay Kit (Promega; Madison, WI) was used in accordance with manufacturer's instructions. Firefly luciferase and *Renilla* luciferase activities were measured with a TD-20/20 Luminometer (Promega, WI).

Western Blot

GMs were homogenized in Tris buffer (10 mM, pH 7.4) containing 1 mM EDTA and protease inhibitors (0.5 mM Pefabloc, 1 uM pepstatin A and 1 mM of each benzamidine and iodoacetamide; Sigma-Aldrich, St. Louis, MO). The homogenates were centrifuged at 1000xg for 10 minutes, and the supernatants were collected and the protein contents were

determined using a DC Protein Assay Kit (Bio-Rad; Hercules, CA) according to manufacturer's instructions. Samples were immunoblotted as described earlier[16,17]: protein samples (40 μg) were electrophoresed through 4–20% acrylamide gels, transferred to PVDF membrane (BioRad; Hercules, CA) and immunoblotted using Atrogin1 and MuRF1 antibodies (ECM BioSciences; Versailles, KY) and an ImmunStar Western Chemiluminescent Kit (Bio-Rad). Optical densities of protein bands were determined using ImageJ (NIH) software.

Study Designs

Study 1—Eight groups of 7 mice each were hindlimb suspended[22] for either 1,2,3,4,5,7,10, or 14 days while another group of 7 weight bearing animals were used as day 0 controls (n=63). After the assigned control or suspension duration, each group of mice was killed according to the approved protocol, and the GMs were harvested and flash frozen in liquid nitrogen. The left GMs from all mice were prepared for real time PCR and thus assayed for expression of *mERG1a*, *MuRF1* and *MAFbx*. Normalized sample C_T values for the Day 0 control were averaged, and the fold increase in gene expression for each gene per mouse was determined by calculating the ratio of each daily sample mouse value to the average Day 0 value.

Study 2—The left legs of 30 (6 groups of 5) mice were injected with 10 μg lacZ and 20 μg empty control expression plasmid, whereas the right legs were injected with a combination of 10 μg lacZ and 20 μg *mERG1a* expression plasmid, and all legs were subjected to electro-transfer. A group of 5 mice each was killed at 1,2,3,4,5, and 6 weeks each after electro-transfer, and the GMs from all legs were harvested and flash frozen in liquid nitrogen. The muscles were cryo-sectioned and stained for lacZ activity as a marker for gene expression. Because a greater abundance (2×) of *mERG1a* than *lacZ* cDNA was injected, we assume that all myofibers staining for lacZ reporter activity also express *mERG1a* and that those myofibers not staining for lacZ activity are not expressing plasmid.

Study 3A—The left GMs of 49 mice (7 groups of 7) were injected with plasmid encoding *lacZ* (10 μg) and a second plasmid encoding *mERG1a* (30 μg), while the right GMs were injected with the *lacZ* plasmid (10 μg) and an empty (control) plasmid (30 μg), followed by electro-transfer. Seven mice were killed immediately to give a Day 0 data point. Seven more mice were killed at days 1,2,3,4,5, and 7 each post electro-transfer. RNA was extracted from GMs, and real time PCR was used to determine expression levels of *mERG1a*, *MuRF1* and *MAFbx*. C_T values were normalized (see methods), and the left (*mERG1a* treatment) to right (control) leg gene expression ratio was determined for each mouse as an indicator of treatment effect. Expression ratios for the Day 0 control were averaged, and the fold increase in gene expression for each gene was determined by calculating the ratio of each daily sample mouse value to the average Day 0 value (baseline).

Study 3B—Ten mice were anesthetized and (as control) the GMs of both legs were injected with: 1) plasmid encoding the *Renilla* luciferase reporter (10 μg), 2) the *MAFbx*/Atrogin1 luciferase reporter plasmid (20 μg), and 3) an empty plasmid (20 μg). The right GMs of another 10 mice were injected as above while the left legs received the same

mixture except that *mERG1a* plasmid (20 μg) was injected instead of the empty plasmid. Seven days after electro-transfer, the GMs were harvested and flash frozen in liquid nitrogen. These were later homogenized and assayed for *Renilla* and firefly luciferase activities using a Dual Luciferase Reporter Kit (ProMega).

Study 4

Hindlimb suspension: Two groups of 3 mice each (n=6) were: 1) allowed to remain weight bearing; or 2) hindlimb suspended. After 7 days of treatment (day 7 is when our model induces significant levels of myofiber CSA decrease[17]), the mice were killed, and the GMs were harvested and used to prepare muscle protein samples (both muscles of 1 mouse composed a sample). Electro-transfer. The GMs of a group of 6 mice (n=6) were injected with DNA (left leg = 10 μg lacZ and 30 μg *mERG1a*; right leg = 10 μg *lacZ* and 30 μg empty control plasmid), and the legs were electroporated. Two muscles were combined to make a sample; that is, 2 left legs made 1 *mERG1a* treated sample, and 2 right legs composed a control sample, etc. GMs of mice from both designs were homogenized and centrifuged as described. Aliquots of each protein sample were electrophoresed and immunoblotted with either MuRF1 or Atrogin1 antibody.

Study 5—Mice (n=56) were assigned randomly to 4 groups (of 16 each), anesthetized, and the left GMs were injected with expression plasmid: 1) *lacZ* (10 μg) and empty plasmid (40 μg); 2) *lacZ* (10 μg), empty (20 μg) and *mERG1* (20 μg); 3) *lacZ* (10 μg), empty plasmid (20 μg) and *HR-FOXO3a* (20 μg); and 4) *lacZ* (10 μg), *mERG1* (20 μg) and *HR-FOXO3a* (20 μg). All right GMs received *lacZ* (10 μg) and control plasmid (20 μg), and all GMs were electroporated. After 7 days, the muscles of 28 mice were assayed for *mERG1a, HR-FOXO3a, MuRF1* and *MAFbx* expression by real time PCR, and the fold increase in gene expression of left leg over right leg was calculated for each mouse. The muscle fiber CSAs were measured in the GMs of the remaining 28 mice.

Statistics

Data were analyzed using either ANOVA or a Student *t*-test as reported in the figure legends. When ANOVA was used, data were analyzed for a completely randomized design. When significant differences were found, means were separated by the Fisher Protected Least Significant Difference. All data were analyzed using the General Linear Model Procedure of SAS (SAS Institute Inc.; Cary, NC). Statements of significance are based on *P*-levels as noted in legends.

RESULTS

Study 1. Hindlimb suspension induces mERG1a, MuRF1, and MAFbx gene expression in the GMs of mice

Rationale—To aid in design of an optimal time course for our *mERG1a* ectopic expression model, we determined the time course of expression for *mERG1a, MuRF1*, and *MAFbx* genes in response to HS. Data. Real time PCR results show that *mERG1a, MuRF1*, and *MAFbx* genes were all expressed in response to HS (Fig. 1). Increases in MAFbx mRNA levels are noted as early as Day1 and continue to increase steeply to reach a maximum at

Day 4. MAFbx mRNA levels begin to decline after Day 4, and expression of this gene is back to Day 1 levels between Days 7 and 10. mERG1a mRNA levels show a mild rise at Day 3 (Fig. 1, inset) just prior to a rise in MuRF1 mRNA levels, which increase sharply between Days 3 and 4 (Figure 1, inset). MuRF1 mRNA levels peak at Day 4 and then drop to initial levels between Days 7 and 10 while mERG1a mRNA levels peak at Day 5 before dropping to initial levels also between Days 7 and 10.

Study 2. Electro-transfer of expression plasmid into mouse GM yields gene transcription and translation with significant results lasting up to 1 month

Rationale—To support the validity of our studies reporting responses (over time) to electro-transfer of expression plasmid into skeletal muscle, we conducted a long term study of changes in GM CSA in response to *mERG1a* expression. *Data*. Indeed, as reported earlier[17], the myofiber CSA was decreased significantly in the myofibers of the *mERG1a* injected legs expressing plasmid relative to the myofibers in the same leg not expressing plasmid and to both the expressing and non-expressing myofibers in muscles injected with *lacZ* and empty plasmid (Fig. 2). The decrease in fiber size is attributable to *mERG1a* expression and is significant for 4 weeks; the *mERG1a* expressing myofiber CSAs are no longer significantly smaller than controls at 5 and 6 weeks after electro-transfer.

Study 3. MuRF1, but not MAXbx, gene expression occurs within the GMs of mice in response to ectopic expression of mERG1a

A. Rationale—To isolate responses to *mERG1a* expression, we ectopically expressed *mERG1a* in GMs of mice and assayed for mRNA of interest over time to ensure that we did not miss changes in expression of the E3 ligase genes. *Data*. Real time PCR results show that indeed *mERG1a* was expressed in response to *mERG1a* plasmid electro-transfer in the GMs (Fig. 3A). Importantly, the *MuRF1* E3 ligase gene was also expressed in response to the *mERG1a* expression and, although no significant differences from baseline transcript levels were detected at Days 1 or 2 post electro-transfer (Fig. 3A), the data reveal that mERG1a and MuRF1 transcript levels both increased above Day 1 levels significantly by Day 3 and peaked at Day 4. Transcript levels for both genes declined toward baseline levels by day 7. The data indicate that *MuRF1* expression is increased by ectopic *mERG1a* expression. Most interestingly, there is no significant increase in *MAFbx* gene expression over the 7 days during which *mERG1a* was expressed, suggesting that ectopic expression of *mERG1a* did not activate this potential route for protein degradation. B. Rationale. To confirm that *mERG1a* expression does not affect *MAFbx* expression, we co-expressed *mERG1a*, a *MAFbx*/Atrogin1 luciferase reporter, and a *Renilla* luciferase reporter (as control for differences in transfection efficiencies) and assayed for dual luciferase activities 7 days later. *Data*. The ratio of firefly to *Renilla* luciferase activities was determined for each leg, and the ratio of luciferase activity in the left to right legs was calculated for each mouse (Fig. 3B). Although mice from a set of positive controls showed that *mERG1a* expression decreases levels of ubiquinated firefly luciferase (data not shown), in concert with expectations, *MAFbx*/Atrogin1 reporter luciferase activity was not altered significantly by *mERG1a* co-expression (Fig. 3B). These studies confirm that *mERG1a* expression does not affect *MAFbx* expression.

Study 4. MuRF1 protein levels increase in response to HS and ectopic expression of mERG1a while Atrogin1 protein levels increase in response to HS only

Rationale—Because increased mRNA expression is not always an indicator of augmented protein synthesis (nor can it be equated with increased protein activity), we assessed levels of MuRF1 and Atrogin1 proteins in GMs from both hindlimb suspended mice and those ectopically expressing *mERG1a* using western blots. *Data*. Both visual observation and optical density data show that MuRF1 protein (~37 kDa) levels increase over controls in the GMs of both HS mice and those ectopically expressing *mERG1a* (Fig. 4A and C, respectively); however, Atrogin1 protein (~41 kDa) levels increase only in response to HS (Fig. 4B,D). The Coomassie stained membranes confirm that equal amounts of protein were loaded into the lanes. These data further demonstrate that *mERG1a* expression induces transcription and translation of *MuRF1*, but not *MAFbx*.

Study 5. Block of FOXO3a DNA binding does not inhibit mERG1a up-regulation of MuRF1

Rationale—To test if MERG1a modulates *MuRF1* expression through FOXO3a, we expressed a mutant form of *FOXO3a* (*HR-FOXO3a*, unable to bind DNA[23]) ± *mERG1a* in WB mice and then assayed for atrophy. If the mERG1a K^+ channel modulates *MuRF1* expression through the FOXO3a transcription factor, then inhibition of active *FOXO3a* DNA binding will lower MuRF1 mRNA levels and diminish the changes in myofiber CSA shown to occur in response to *mERG1a* expression[17]. Data. The fold increase in mERG1a and FOXO3a mRNA levels in muscles injected with each respective expression plasmid shows that transcripts were made (Fig. 5A). The data also show that the MuRF1 mRNA level was significantly increased in response to *mERG1a* expression and confirm that MAFbx mRNA levels are not affected by *mERG1a* expression or by the levels of *MuRF1* expression reached in this experiment. It further shows that *mERG1a* expression did not result in increased levels of *FOXO3a* transcription, because our primers would have detected this native mRNA. Although statistically insignificant, the fold increases in MAFbx transcript do “creep” above 1.0, hinting that the *HR-FOXO3a* product could be inhibiting some basal level of *MAFbx* transcription. Most interestingly, there was no significant change in the levels of mERG1a-induced MuRF1 mRNA transcribed in the presence of HR-FOXO3a as would be expected if mERG1a modulated *MuRF1* transcription through FOXO3a (Fig. 5A). Muscle fiber CSA data demonstrate that, indeed, muscle fiber size decreases in response to *mERG1a* expression; however, this decrease in muscle fiber CSA is not affected by expression of *HR-FOXO3a* (Fig. 5B). These sets of data suggest that mERG1a does not modulate *MuRF1*expression through FOXO3a activity. *Verification:* To ensure the validity of experiments performed with *HR-FOXO3a*, we determined that the *HR-FOXO3a* plasmid functions as a dominant negative when ectopically expressed in mouse GM. We ectopically expressed empty control plasmid (40 μg) in the right legs of 20 mice. The left legs of 10 of these mice received the same plasmid as control while another group of 10 received *HR-FOXO3a* (40 μg) in their left legs. All mice were hindlimb suspended. After 4 days, we harvested the GMs, determined the MAFbx mRNA expression levels using real time PCR, and analyzed the data to yield ratios of MAFbx mRNA expression in left to right legs. As expected, HS resulted in increased *MAFbx* expression over weight bearing controls. The ratio of MAFbx mRNA expression in the control mice (left over right leg) was

1.06 ±0.06, while the ratio was 0.8±0.08 ($P \leq 0.05$) in the mice receiving the *HR-FOXO3a* plasmid in their left legs, indicating the inactive *HR-FOXO3a* gene product interfered with transcription of *MAFbx* in muscle of HS mice as would be expected.

DISCUSSION

In earlier work, we showed that the mERG1a K^+ channel is up-regulated in atrophic GM from hindlimb suspended mice in contrast to muscle from weight bearing control animals and that mERG1a up-regulates UPP activity[17]. The mechanism(s) by which mERG1a modulate(s) UPP activity are unknown. We hypothesize that mERG1a acts upstream of pathways already known to modulate the UPP in SKM atrophy. For example, it has been shown that deactivation of the PI3K/AKT1/FOXO pathway and/or activation of the IKK-β/IκB-α/NF-κB pathway can up-regulate UPP activity in atrophic SKM mainly by modulating expression of "atrogenes" (i.e., genes up-regulated during muscle loss). Particularly, these pathways have been shown to up-regulate genes which encode the SKM specific E3 ligases, MuRF1 and Atrogin1[1,2,7]. In fact, recent studies demonstrate that both FOXO and NF-κB transcription factors are up-regulated in many atrophy models (including unloading),[20,24–26] and a particularly elegant study by Reed and colleagues demonstrates that each of these transcription factor families is responsible for roughly 50% of the muscle loss occurring in immobilization-induced atrophy[12]. Here we report that hindlimb suspension induces atrophy and up-regulates expression of *mERG1a*, *MuRF1*, and *MAFbx* genes and, interestingly, that ectopic expression of the mERG1a K^+ channel in mouse GM increases expression of the *MuRF1* gene, but not that of the *MAFbx* gene. We hypothesize, therefore, that although mERG1a could act on *MuRF1* gene expression through a novel pathway, it likely modulates *MuRF1* expression by a pathway currently known to modulate E3 ligase expression.

PI3K/Akt/FOXO

In general, deactivation of PI3K (phosphoinositide 3-kinase) results in reduced Akt phosphorylation and, thereby, deactivation of this enzyme. Once deactivated, Akt no longer phosphorylates FOXO transcription factors; the dephosphorylated/activated FOXO (3 isoforms have been described in SKM: FOXO1, 3, and 4) then moves to the nucleus and promotes transcription of *MAFbx* and/or *MuRF-1* and other known atrogenes[1,2,7]. Research with diabetes–induced muscle atrophy suggests that UPP activity is increased by suppressed PI3K and Akt activities with concomitant increased FOXO1 phosphorylation and resultant increases in MAFbx and MuRF1 mRNA levels[27–29]. In dexamethasone treated C2C12 myotubes, it has been shown that FOXO1 does not increase *MuRF1* or *MAFbx* transcription directly but does so indirectly by inhibiting the IGF-1 block of their upregulation[30]. It has been demonstrated that *FOXO3a* expression results in increased levels of MuRF1 mRNA[31] in cardiomyocytes and also induces transcription of *MAFbx*[20]. In immobilization studies, upregulation of *MAXbx* and *MuRF1* expression occurs in numerous species including mice[32] and rats[8,33]. Unloading studies in humans also reveal changes in *MuRF1* and *MAFbx* expression[34] and show that these changes differ according to which muscle is monitored and suggest, therefore, that E3 ligase expression may be fiber type specific[4,35]. Nonetheless, the mechanism(s) responsible for these changes in E3 ligase abundances are not well understood.

Here we show that hindlimb suspension induces expression of *mERG1a*, *MuRF1*, and *MAFbx*. In fact, transcription of all the assayed genes occurs early in HS prior to Day 7, at which time muscle fiber CSA is significantly smaller than in control WB mice[17]. However, while MuRF1 mRNA levels are correlated with *mERG1a* expression, MAFbx mRNA levels begin to rise prior to any noted increase in mERG1a mRNA levels, suggesting that at least initial *MAFbx* gene expression is likely not linked to HS induced *mERG1a* expression. Importantly, we demonstrate that ectopic expression of *mERG1a* indeed induces expression of *MuRF1* in mouse GM. In fact, *MuRF1* expression mirrors that of electro-transferred *mERG1a* very closely, with mERG1a levels rising at day 3 prior to a sharp increase in MuRF1 mRNA levels between Days 3 and 4. These data suggest that the increase in *MuRF1* expression is likely subsequent to the day 3 rise in mERG1a transcript. Interestingly, data also show that *mERG1a* expression does not induce *MAFbx* transcription. This is most interesting, because this isolation of *mERG1a*-expression effects reveals a separation of E3 ligase modulation at the level of a membrane protein. Because it has been shown that FOXO3a induces expression of *MAFbx* specifically by binding directly to the *MAFbx* promoter in mouse muscle[21], our data suggest that mERG1a does not modulate *FOXO3a* gene expression or protein activity. To test if mERG1a affects *MuRF1* expression through FOXO3a, we co-expressed *mERG1a* and an inactive *FOXO3a* (*HR-FOXO3a*). We found that inhibition of FOXO3a activity (i.e., DNA binding) did not diminish changes shown to occur in response to *mERG1a* expression. That is, it did not lower MuRF1 mRNA levels or prevent the decrease in muscle fiber CSA seen in *mERG1a* treated controls. Further, our studies reveal that *mERG1a* expression does not modulate FOXO3a mRNA levels. Therefore, we conclude that MERG1a does not induce *MuRF1* transcription through up-regulation of *FOXO3a* expression. Further, we suggest that it is not likely that MERG1a induces FOXO3a activity (increased inhibition of its phosphorylation or increased dephosphorylation), mainly because MAFbx mRNA levels do not increase with *mERG1a* expression as would be expected if FOXO3a activation were augmented and translocation to the nucleus were up-regulated. (Of course, our data do not rule out the possibility that mERG1a up-regulation of *MAFbx* transcription requires some *MAFbx* promoter specific co-factor not present in this model, but present during HS, which would allow FOXO3a to bind the *MAFbx* promoter.) It still remains to be determined definitively if the mERG1a channel modulates *MuRF1* expression through the FOXO transcription factor family. We suspect that mERG1a does not affect FOXO factors because: 1) it does not modulate *MAFbx* expression (and it has been shown that FOXO 1 and 4 can modulate *MAFbx* expression in some models[30,36]); and 2) increasingly, research suggests that *MAFbx* expression is modulated by FOXO transcription factors while *MuRF1* expression is regulated by NF-kB factors[20,21,36,37]. Nonetheless, further studies with mutant forms of FOXO1 and FOXO4 should be performed to determine definitively that mERG1a is (or is not) inducing *MuRF1* expression through these transcription factors. If FOXO family members are implicated, then studies determining if Akt and PI3K are involved will be required.

Other recent work reports that treatment of rat skeletal muscle with PPAR-α agonist yields decreased PI3K/Akt signaling activity, increased *FOXO1* transcription factor activity, and concomitant increases in *MuRF1* and *MAFbx* expression[38]. If mERG1a is increasing MuRF1 production by inactivating some point of the PI3K/Akt pathway, then it could be

acting through effects of PPAR-α agonists on the membrane-bound PPAR-α receptors. Of course, the work does not address potential effects on other pathways (e.g., NF-κB factors), so it does not rule out that PPAR-α activation is increasing *MuRF1* (or *MAFbx*) expression through other activity(-ies). PI3K/Akt independent mechanisms also have been shown to modulate FOXO activity. For example, Nemo-like kinase (NLK) has been shown to bind and phosphorylate FOXO1, thereby inhibiting its transcriptional activity through the PI3k/Akt independent transforming growth factor-beta-activated kinase (TAK1)-NLK pathway[39]. Further, *Atrogin1* expression has been shown to be induced by a p38MAPK dependent pathway in cardiac myocytes, independent of the Akt/FOXO pathway[40]. These routes represent further possibilities for mERG1a modulation of *MuRF1* expression.

IKK-β/IκB-α/NF-κB

Activation of NF-κB family members by upstream IKK-β activation leads to production of E3 ligases[2,24,37,41]. In brief, some factor triggers activation of IKK-β (kinase) by phosphorylation. In cachectic atrophy, evidence suggests that activation of tumor necrosis factor alpha receptors triggers this step, but this does not appear to be the case with atrophy induced by unloading. In both cases, however, active IKK-β phosphorylates IκB-α, which is then ubiquitinated and degraded, releasing bound NF-κB factors. Different NF-κB factors are released dependent upon what triggers the atrophy[1]. In unloading atrophy, it has been shown that levels of p50 (NF-κB factor) and Bcl-3 (an IκB family member) increase with atrophic conditions and, in fact, the decrease in SKM size caused by hindlimb suspension is ameliorated in both p50 and Bcl-3 knockout mice[26]. Once released, the NF-κB proteins then translocate to the nucleus and cause transcription of numerous genes, including *MuRF1*, but interestingly, not *MAFbx*[37,41]. We suggest, in fact, that because ectopic expression of *mERG1a* induces an increase in MuRF1 (and not MAFbx) mRNA and protein levels, that mERG1a would modulate (increase) the expression and/or activity of upstream *NF-κB* transcription factors. Nonetheless, given that *mERG1a* expression causes a significant increase in MuRF1 mRNA and protein levels and the fact that NF-κB factors are known to be involved in *MuRF1* expression, the data suggest that mERG1a could modulate NF-κB factor expression and/or activity. Identifying if/which NF-κB factors are modulated by mERG1a and the mechanism(s) by which this occurs clearly requires study.

In summary, we present data which show that *MuRF1* gene expression is significantly increased in response to *mERG1a* expression and confirms that *MAFbx* expression is not affected by *mERG1a* expression or by the levels of MuRF1 reached in these experiments. That is, we have shown what appears to be a complete separation of MuRF1 and *MAFbx*/Atrogin1 E3 ligase modulation at the level of a membrane protein. Further, we demonstrate that *MuRF1* modulation by mERG1a is not occurring through FOXO3a. Considering our data, this latter conclusion is not surprising, given the fact that NF-κB is basically required for disuse muscle atrophy[27,37,42] and that *MuRF1*, and not *MAFbx*, transcription is increased by NF-κB factors[37]. Obviously, the mechanism by which the mERG1a K^+ channel up-regulates *MuRF1* expression in SKM needs further investigation along with the factors inducing up-regulation of the K^+ channel itself. Investigation of the mechanism(s) initiating SKM atrophy is important, because SKM atrophy is coincident with many pathological conditions and is related to increased disability, morbidity, and mortality, and understanding

these pathways will suggest specific, more effective therapies for abatement of this debilitating condition.

Acknowledgments

The authors wish to thank Dr. Barry London (Cardiovascular Institute, Univ. of Pittsburgh, PA) for his generous gifts of the *mERG1a* and *DN-mERG1a* clones in pBK/CMV. Appreciation is also expressed to Dr. Stewart Lecker (Beth Israel Deaconess Medical Center, Boston, MA) for kindly providing the *MAFbx*/Atrogin1 luciferase reporter. Research reported in this publication was supported by the National Institute of Arthritis and Musculoskeletal and Skin Diseases of the National Institutes of Health under Award Number NIH NIAMS 1R03AR053706-01A2 to ALP. The content is solely the responsibility of the authors and does not necessarily represent the official views of the National Institutes of Health.

ABBREVIATIONS

SKM	skeletal muscle
UPP	ubiquitin proteasome proteolysis
E3 ligase	ubiquitin protein ligase
MAFbx	Muscle atrophy F-box
MuRF1	Muscle RING Finger-1
SCF	Skp1, cdc53/Cullin and F-box protein
NF-κB	Nfkappa B
ERG1a	ether-a-gogo-related gene 1a
mERG1a	mouse ether-a-gogo-related gene 1a
HERG1A	human ether-a-gogo-related gene 1A
HS	hindlimb suspension
GM	gastrocnemius muscle
WB	weight bearing
WT	wildtype
DN-mERG1a	dominant negative mERG1a
CSA	cross sectional area
lacZ	β-galactosidase enzyme

REFERENCES

1. Kandarian SC, Jackman RW. Intracellular signaling during skeletal muscle atrophy. Muscle Nerve. 2006; 33:155–165. [PubMed: 16228971]
2. Foletta VC, White LJ, Larsen AE, Leger B, Russell AP. The role and regulation of MAFbx/atrogin-1 and MuRF1 in skeletal muscle atrophy. Pflugers Arch–Eur J Physiol. 2011; 461:325–335. [PubMed: 21221630]
3. Kamei Y, Miura S, Suzuki M, Kai Y, Mizukami J, Taniguchi T, et al. Skeletal muscle FOXO1 (FKHR) transgenic mice have less skeletal muscle mass, down-regulated type I (slow twitch/red muscle) fiber genes and impaired glycemic control. J Biol Chem. 2004; 279:41114–41123. [PubMed: 15272020]

4. Salanova M, Schiffl G, Puttman B, Schoser BG, Blottner D. Molecular biomarkers monitoring human skeletal muscle fibres and microvasculature following long-term bed rest with and without countermeasures. J Anat. 2008; 212:306–318. [PubMed: 18221329]
5. Lecker SH, Solomon V, Mitch WE, Goldberg AL. Muscle protein breakdown and the critical role of the ubiquitin-proteasome pathway in normal and disease states. J Nutri. 1999; 129:227–237.
6. Glass DJ. Signalling pathways that mediate skeletal muscle hypertrophy and atrophy. Nature Cell Biol. 2003; 5:87–90. [PubMed: 12563267]
7. Franch HA, Price SR. Molecular signaling pathways regulating muscle proteolysis during atrophy. Curr Opin Clin Nutr Metab Care. 2005; 8:271–275. [PubMed: 15809529]
8. Bodine SC, Latres E, Baumhueter S, Lai VK, Nunez L, Clarke BA, et al. Identification of ubiquitin ligases required for skeletal muscle atrophy. Science. 2001; 294:1704–1708. [PubMed: 11679633]
9. Gomes MD, Lecker SH, Jagoe RT, Navon A, Goldberg AL. Atrogin-1, a muscle-specific F-box protein highly expressed during muscle atrophy. Proc Natl Acad Sci USA. 2001; 98:14440–14445. [PubMed: 11717410]
10. Zhang P, Chen X, Fan M. Signaling mechanisms involved in disuse muscle atrophy. Med Hypotheses. 2007; 69:310–321. [PubMed: 17376604]
11. Joazeiro CA, Weismann AM. RING finger proteins: mediators of ubiquitin ligase acitivity. Cell. 2000; 102:549–552. [PubMed: 11007473]
12. Reed SA, Senf SM, Cornwell EW, Kandarian SC, Judge AR. Inhibition of IkappaB alpha (IKKα) or IKKbeta (IKKβ) plus forkhead box O (Foxo) abolishes skeletal muscle atrophy. Biochem Biophy Res Comm. 2011; 405:491–496.
13. Curran ME, Splawski I, Timothy KW, Vincent GM, Green ED, Keating MT. A molecular basis for cardiac arrhythmia: *herg* mutations cause long QT syndrome. Cell. 1995; 80:795–803. [PubMed: 7889573]
14. Lees-Miller JP, Kondo C, Wang L, Duff HJ. Electrophysiological characterization of an alternatively processed ERG K+ channel in mouse and human hearts. Circ Res. 1997; 81(5):719–726. [PubMed: 9351446]
15. London B, Trudeau MC, Newton KP, Beyer AK, Copeland NG, Gilbert DJ, et al. Two isoforms of the mouse Ether-a-go-go-related gene coassemble to form channels with properties similar to the rapidly activating component of the cardiac delayed rectifier K^+ current. Circ Res. 1997; 81:870–878. [PubMed: 9351462]
16. Pond AL, Scheve BK, Benedict AT, Petrecca K, Van Wagoner DR, Shrier A, et al. Expression of distinct ERG proteins in rat, mouse and human heart. J Biol Chem. 2000; 275(8):5997–6006. [PubMed: 10681594]
17. Wang X, Hockerman GH, Green HW 3rd, Babbs CF, Mohammad SI, Gerrard D, et al. Merg1a K^+ channel induces skeletal muscle atrophy by activating the ubiquitin proteasome pathway. FASEB J. 2006; 20(9):1531–1533. [PubMed: 16723379]
18. Selyanko AA, Delmas P, Hadley JK, Tatulian L, Wood IC, Mistry M, et al. Dominant-negative subunits reveal potassium channel families that contribute to M-like potassium currents. J. Neurosci. 2002; 22:RC212–RC217. [PubMed: 11880533]
19. Taylor JA, Babbs CF, Alzghoul MB, Olsen A, Latour MA, Pond AL, et al. Optimization of Ectopic Gene Expression in Skeletal Muscle through DNA Transfer by Electrotransfer. BMC Biotechnology. 2004; 4:11. [PubMed: 15149549]
20. Sandri M, Sandri C, Gilbert A, Skurk C, Calabria E, Picard A, et al. Foxo transcription factors induce the atrophy-related ubiquitin ligase atrogin-1 and cause skeletal muscle atrophy. Cell. 2004; 117:399–412. [PubMed: 15109499]
21. Sandri M, Lin J, Handschin C, Yang W, Arany ZP, Lecker SH, et al. PGC-1α protects skeletal muscle from atrophy by suppressing Fox03 action and atrophy-specific gene transcription. Proc Natl Acad Sci USA. 2006; 103:16260–16265. [PubMed: 17053067]
22. Alzghoul MB, Gerrard D, Watkins BA, Hannon K. Ectopic expression of IGF-1 and Shh by skeletal muscle inhibits disuse-mediated skeletal muscle atrophy and bone osteopenia in vivo. FASEB J. 2004; 18:221–223. [PubMed: 14597562]
23. Katayama K, Nakamura A, Sugimoto Y, Tsuruo T, Fujita N. FOXO transcription factor-dependent p15ink14 and p19ink4d expression. Oncogene. 2008; 27:1677–1686. [PubMed: 17873901]

24. Hunter RB, Stevenson E, Koncarevic A, Mitchell-Felton H, Essig DA, Kandarian SC. Activation of an alternative NF-kappaB pathway in skeletal muscle during disuse atrophy. FASEB J. 2002; 16:529–538. [PubMed: 11919155]
25. Van Gammeen D, Damrauer JS, Jackman RW, Kandarian SC. The IkappaB kinases IKKalpha and IKKbeta are necessary and sufficient for skeletal muscle atrophy. FASEB J. 2009; 23:362–370. [PubMed: 18827022]
26. Hunter RB, Kandarian SC. Disruption of either the Nfkb1 or the Bcl3 gene inhibits skeletal muscle atrophy. J Clin Invest. 2004; 114:1504–1511. [PubMed: 15546001]
27. Dehoux M, van Beneden R, Pasko N, Lause P, Verniers J, Underwood L, et al. Role of the insulin-like growth factor I decline in the induction of atrogin-1/MAFbx during fasting and diabetes. Endocrinology. 2004; 145:4806–4812. [PubMed: 15284206]
28. Wang X, Hu Z, Hu J, Du J, Mitch WE. Insulin resistance accelerates muscle protein degradation: activation of the ubiquitin-proteaseome pathway by defects in muscle cell signaling. Endocrinology. 2006; 147:4160–4168. [PubMed: 16777975]
29. Waddell DS, Baehr LM, van den Brandt J, Johnsen SA, Reichardt HM, Furlow JD, et al. The glucocorticoid receptor and FOXO1 synergistically activate the skeletal muscle atrophy-associated MuRF1 gene. Am J Physiol Endocrinol Metab. 2008; 295:E785–E797. [PubMed: 18612045]
30. Stitt TN, Drujan D, Clarke BA, Panaro F, Timofeyva Y, Kline WO, et al. The IGF-1/PI3K/Akt pathway prevents expression of muscle atrophy-induced ubiquitin ligases by inhibiting FOXO transcription factors. Mol Cell. 2004; 14:395–403. [PubMed: 15125842]
31. Skurk C, Izumiya Y, Maatz H, Razeghi P, Shiojima I, Sandri M, et al. The FOXO3a transcription factor regulates cardiac myocyte size downstream of AKT signaling. J Biol Chem. 2005; 280:20814–20823. [PubMed: 15781459]
32. Caron AZ, Drouin G, Desrosiers J, Trensz F, Grenier G. A novel hindlimb immobilization procedure for studying muscle atrophy and recovery in mice. J Appl Physiol. 2009; 106:2049–2059. [PubMed: 19342435]
33. Haddad F, Adams GR, Bodell PW, Baldwin KM. Isometric resistance exercise fails to counteract skeletal muscle atrophy processes during the initial stages of unloading. J Appl Physiol. 2006; 100:433–441. [PubMed: 16239603]
34. Gustafsson T, Osterlund T, Flanagan JN, von Walden F, Trappe TA, Linnehan RM, et al. Effects of 3 days unloading on molecular regulators of muscle size in humans. J Appl Physiol. 2010; 109:721–727. [PubMed: 20538844]
35. Jones SW, Hill RJ, Krasney PA, O'Conner B, Peirce N, Greenhaff PL. Disuse atrophy and exercise rehabilitation in humans profoundly affects the expression of genes associated with the regulation of skeletal muscle mass. FASEB J. 2004; 18:1025–1027. [PubMed: 15084522]
36. Moylan JS, Smith JD, Chambers MA, McLoughlin TJ, Reid MB. TNF induction of atrogin-1/MAFbx mRNa depends on Foxo4 expression but not AKT-Foxo1/3 signaling. Am J Physiol Cell Physiol. 2008; 295:C986–C993. [PubMed: 18701653]
37. Cai D, Frantz JD, Tawa NE Jr, Melendez PA, Oh B-C, Lidov HGW, et al. IKKβ/NF-κB activation causes severe muscle wasting in mice. Cell. 2004; 119:285–298. [PubMed: 15479644]
38. Ringseis R, Keller J, Lukas I, Spielmann J, Most E, Couturier A, et al. Treatment with pharmacological PPARα agonists stimulates the ubiquitin proteasome pathway and myofibrillar protein breakdown in skeletal muscle of rodents. Biochim Biophys Acta. 2013; 1830(1):2105–2117. [PubMed: 23041501]
39. Kim S, Kim Y, Lee J, Chung J. Regulation of FOXO1 by TAK1-Nemo-like kinase pathway. J Biol Chem. 2010; 285(11):8122–8129. [PubMed: 20061393]
40. Yamamoto Y, Hoshino Y, Ito T, Nariai T, Mohri T, Obana M, et al. Atrogin-1 ubiquitin ligase is upregulated by doxorubicin via p38-MAP kinase in cardiac myocytes. Cardiovasc Res. 2008; 79(1):89–96. [PubMed: 18346979]
41. Dodd SL, Hain B, Senf SM, Judge AR. Hsp27 inhibits IKKβ-induced NF-κB activity and skeletal muscle atrophy. FASEB J. 2009; 23:3415–3423. [PubMed: 19528257]
42. Judge AR, Koncarevic A, Hunter RB, Liou HC, Jackman RW, Kandarian SC. Role for IkappaBalpha, but not c-Rel, in skeletal muscle atrophy. Am J Physiol cell Physiol. 2007; 292:C372–C382. [PubMed: 16928772]

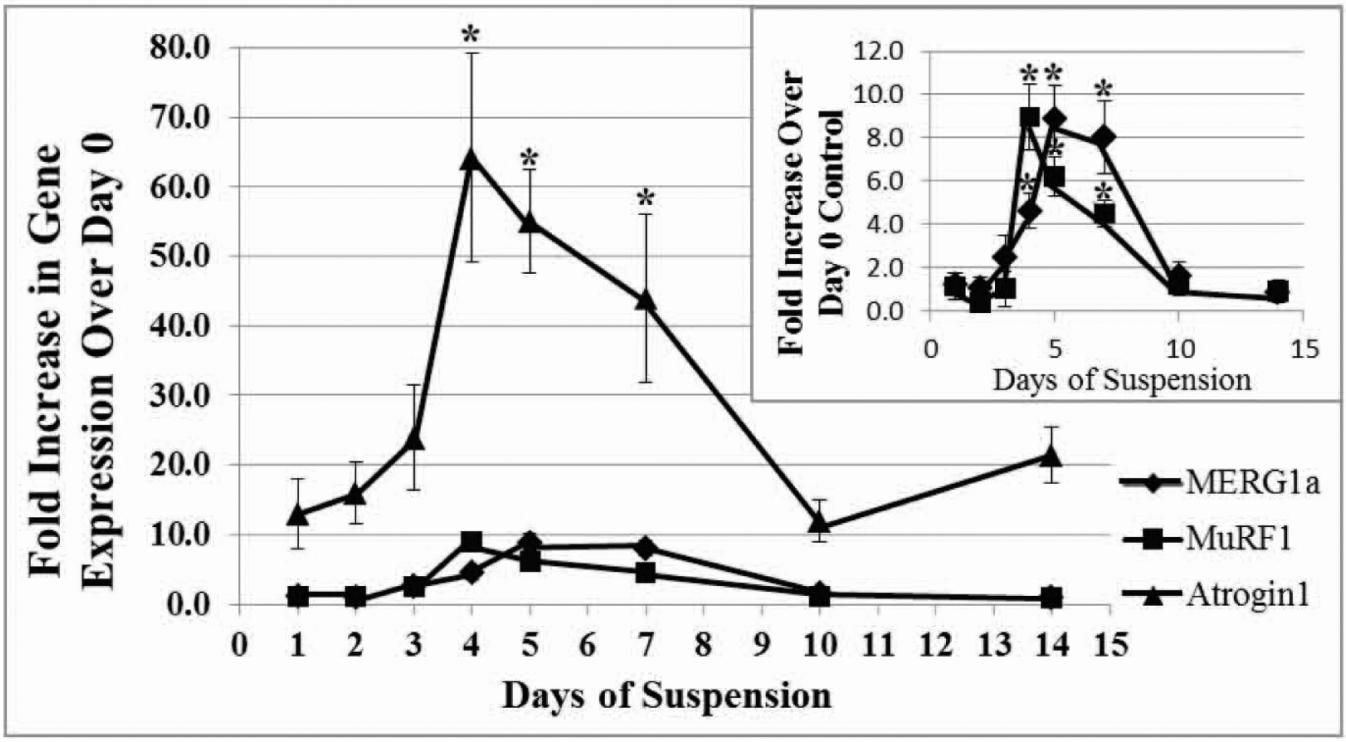

Figure 1.

Hindlimb suspension (HS) induces *mERG1a, MuRF1*, and *MAFbx* gene expression in the gastrocnemius muscle of mice. Real time PCR demonstrates that HS induces highest expression of *mERG1a, MuRF1*, and *MAFbx* genes soon after commencement of suspension. Each daily data point was compared to the average day 0 level (day X/day 0) to yield a fold increase per mouse; fold increase per mouse data were averaged per day. Data points are, therefore, mean fold increase in gene expression (± standard deviation) over time. Inset: *mERG1a* and *MuRF1* gene expression is graphed using a smaller y-axis to better show response to time course. Within gene, all data were analyzed by ANOVA (see methods). *Significant (P<0.05) increase in gene expression over the day 0 control within gene. 7 mice/day, n=63 mice.

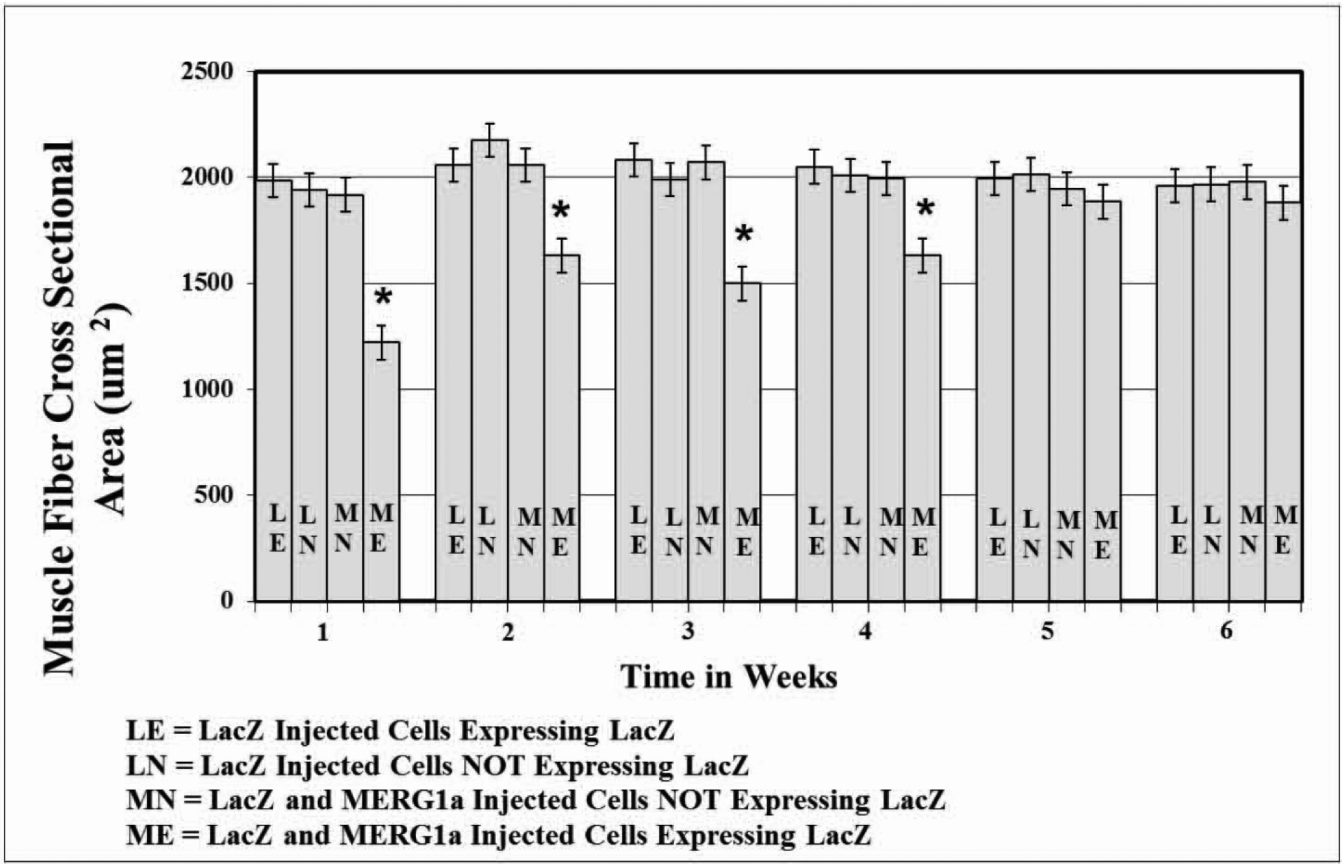

Figure 2.

Electro-transfer of *mERG1a* and the *lacZ* reporter expression plasmids into gastrocnemius muscle (GM) yields results lasting 4 weeks. Relative to fibers of muscles injected with *mERG1a* and β-*galactosidase* (*lacZ*), but not expressing *lacZ* activity (MN), the cross sectional areas of the fibers injected with *mERG1a* and expressing *lacZ* activity (ME) are decreased significantly in weeks 1 through 4. The areas of the ME fibers are also significantly smaller than *lacZ* expressing (LE) and non-expressing (LN) fibers of GMs injected with *lacZ* only. There are no significant differences in fiber cross sectional area after 4 weeks. All data were analyzed by ANOVA (see methods). **P*<0.05, n=30 mice.

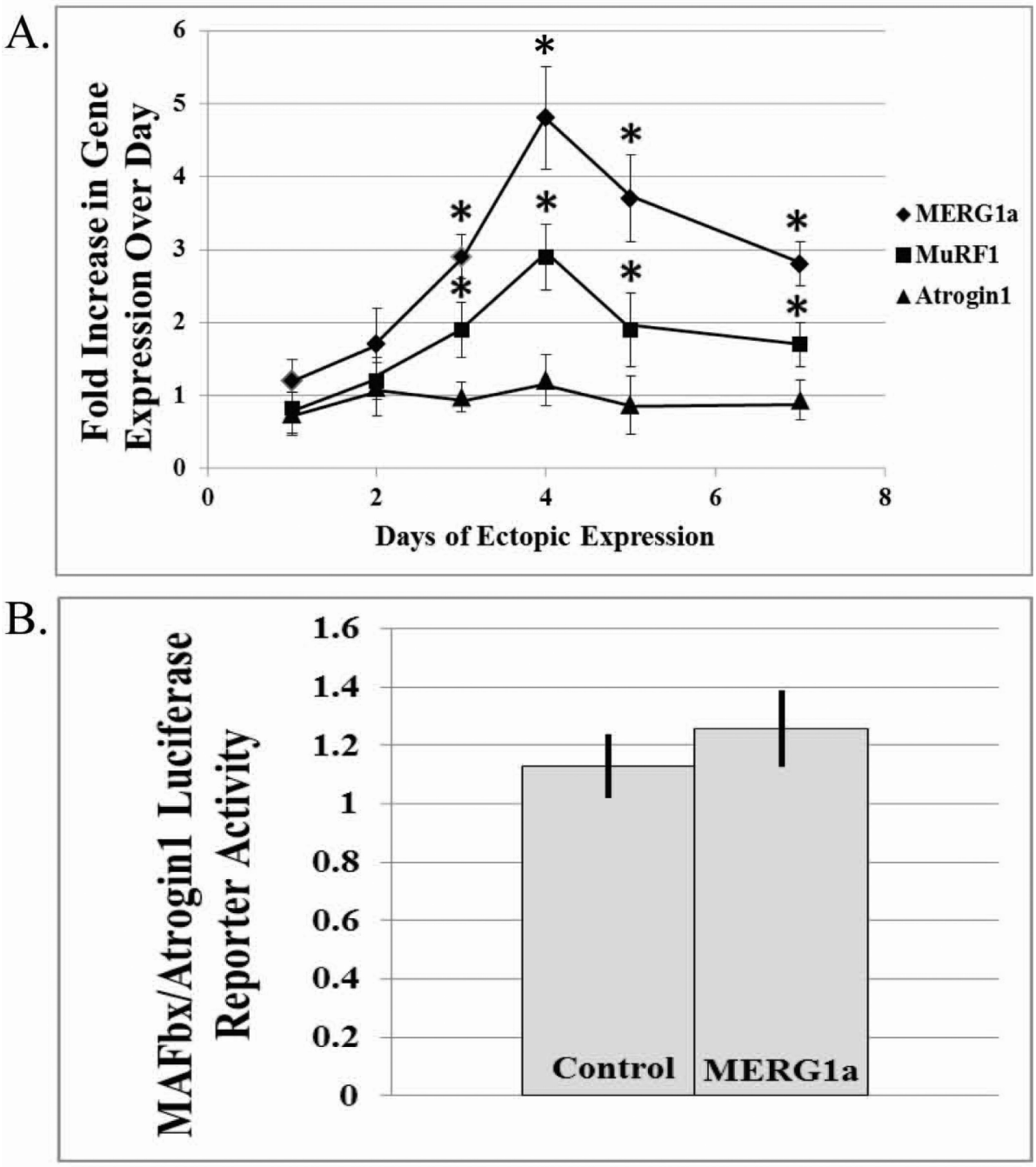

Figure 3.

MuRF1, but not *MAFbx*, gene expression occurs within mouse gastrocnemius muscles (GM) in response to *mERG1a* expression. A. mERG1a and MuRF1 mRNA levels increase in response to *mERG1a* electro-transfer. Methods. Left GMs were injected with β-*galactosidase* (*lacZ*) and *mERG1a* plasmids; right GMs received *lacZ* and empty plasmid. After electro-transfer, GMs from 7 mice were harvested each day at days 0–5,7 and assayed with real time PCR. Data represent mean (± SD) fold increase in daily gene expression over average day 0. Within gene, data were analyzed by ANOVA. *significant (P<0.05) increase

in expression over day 0 within gene, 7 mice/day, n=49. B. *mERG1a* expression in GM does not modulate *MAFbx* expression. Right GMs (n=20) were injected with: 1) *Renilla* luciferase reporter, 2) *MAFbx*/Atrogin1 luciferase reporter, and 3) empty plasmid. Left GMs were treated identically, except they received *mERG1a* instead of empty plasmid. Seven days post electro-transfer, GMs were assayed using a Dual Luciferase Reporter Kit (ProMega). The ratio of firefly to *Renilla* luciferase activities was determined per leg, and activity ratios (left to right legs) were calculated per mouse. Data were analyzed by Student *t*-test and represent mean ± SD; $P<0.55$.

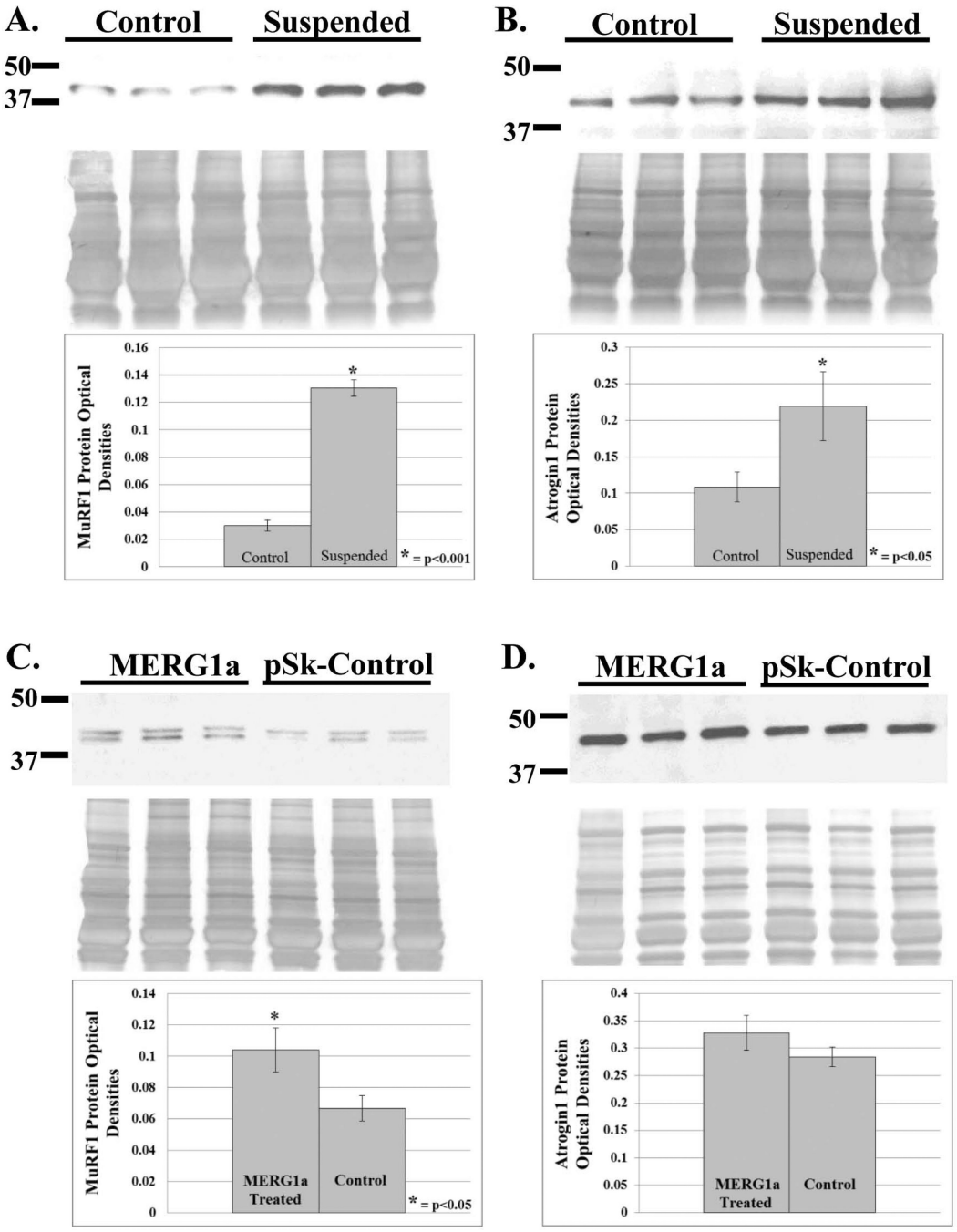

Figure 4.

Immunoblots demonstrate that MuRF1 protein levels in gastrocnemius muscles (GMs) increase in response to both hindlimb suspension (HS) and ectopic expression of *mERG1a*, while Atrogin1 protein levels increase in response to HS only. Protein samples (40 μg) from GMs were electrophoresed through 4–20% acrylamide gels, transferred to PVDF membrane (BioRad; Hercules, CA) and immunoblotted with antibody recognizing either MuRF1 or Atrogin1 protein (ECM BioSciences; Versailles, KY). A and B. In both immunoblots (top), lanes 1–3 contain control GMs, while lanes 4–6 contain GMs from mice suspended for 4

days. MuRF1 (A) and Atrogin1 (B) protein levels increased significantly (434% and 222%, respectively) in response to HS. C and D. In both immunoblots (top), lanes 1–3 contain GMs electro-transferred with *mERG1a*, while lanes 4–6 contain GMs electro-transferred with control plasmid. MuRF1 protein levels (C) increased significantly (156%), while the increase (115%) in Atrogin1 protein abundance (D) is not significant. A–D. Coomassie stained membranes (below immunoblots) show that equivalent levels of protein were loaded into the lanes. Data were analyzed by Student *t*-test. Bars represent the mean (± SD) optical density units of proteins as determined by ImageJ (NIH). The *P*-values are noted in the graphs.

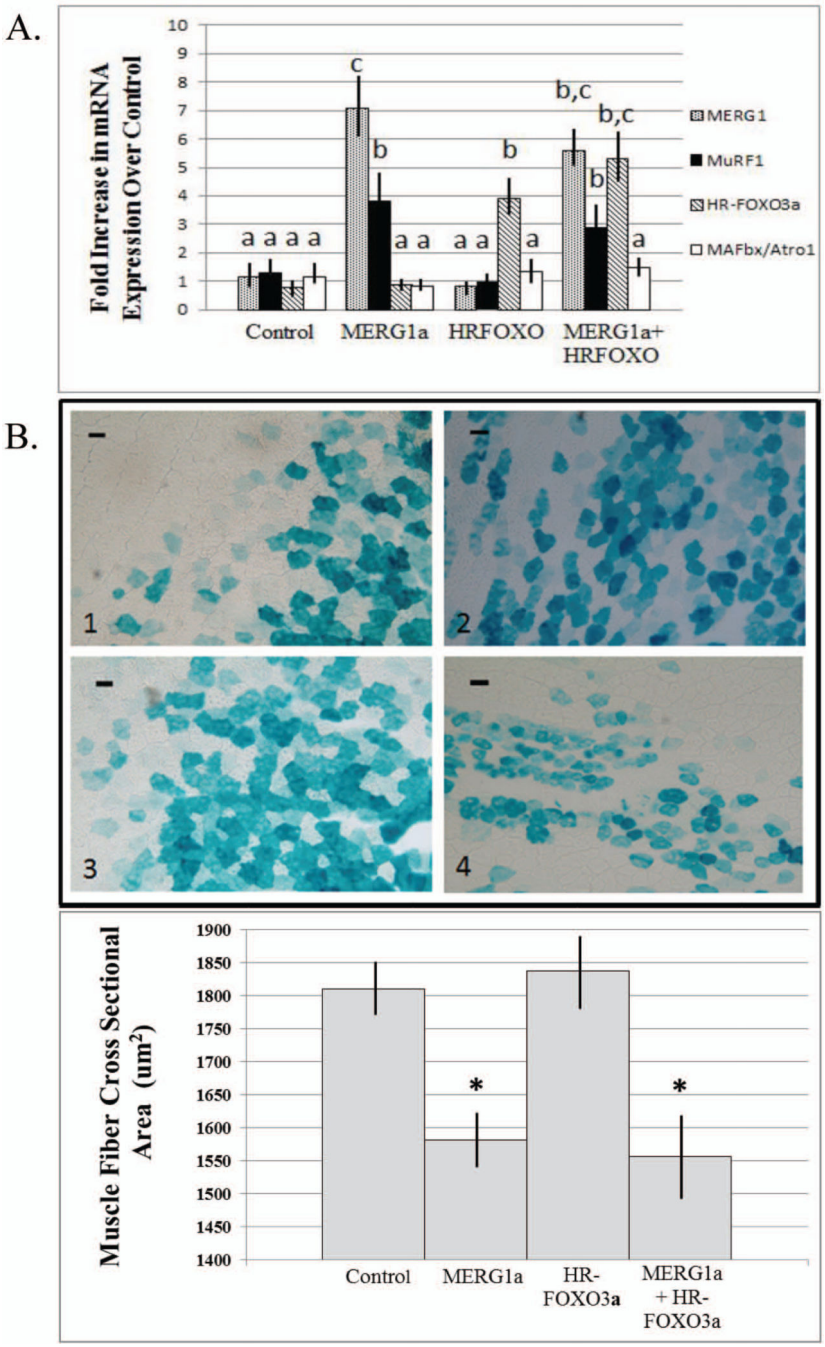

Figure 5.

mERG1a-induced up-regulation of *MuRF1* expression is not inhibited by block of FOXO3a DNA binding. We expressed *HR-FOXO3a* (an inactive mutant unable to bind DNA) ± *mERG1a* in mouse gastrocnemius muscle (GM) and assayed for atrophy: A. E3 ligase expression; and B. muscle fiber cross sectional area (CSA). *A.* Real time PCR indicates that the increase in *MuRF1* mRNA levels noted in response to *mERG1a* expression is not curtailed by co-expression of *HR-FOXO3a*. Further, ectopic *mERG1a* expression does not affect levels of FOXO3a nor MAFbx mRNA. Data were analyzed by ANOVA and are

expressed as group mean ± SEM. Different letters indicate significant differences, $P \leq 0.05$, n=28 mice. *B*. The decrease in muscle fiber CSA that occurs in response to *mERG1a* expression is not affected by co-expression of *HR-FOXO3a*. GMs were injected with expression plasmids: 1. control and β-*galactosidase* (*lacZ*); 2. control, *lacZ* and *mERG1a*; 3. control, *lacZ* and *HR-FOXO3a*; and 4. *lacZ*, *mERG1a* and *HR-FOXO3a*. Seven days after electro-transfer, muscle cryosections were stained for lacZ reporter to indicate plasmid expression. Data were analyzed by ANOVA. Bars represent mean CSA ± SEM. *$P \leq 0.01$, n=28. Scale bar = 40 μm.

Table 1

Forward and reverse primers used for real time PCR.

Target Gene	TM °C	Forward Primer	Reverse Primer	Amplicon
mERG1a	60	5'–CGC AGA ACA CCT TCC TCG ACA C-3'	5'–GCA GAA GCC GTC GTT GCA GTA G-3'	119 bp
MuRF1	55	5'–GGG CTA CCT TCC TCT CAA GTG–3'	5'–ACT CCT CCT CCT CCT CAT CTG–3'	183 bp
MAFbx	55	5'–CGT CGC AGC CAA GAA GAG AAA G–3'	5'–ATC CAG GAT GGC AGT CGA GAA G–3'	171 bp
FOXO3a	70 f; 60 r	5'-AAA TGT TCG TCG CGG CGG AAC-3'	5'–GTC GCC CTT ATC CTT GAA GTA–3'	153 bp
18S (ribosomal)	57 f; 58 r	5'–CGG CTA CCA CAT CCA AGG AA–3'	5'–GCT GGA ATT ACC GCG GCT–3'	123 bp